\$ SUPER

Contents lists available at ScienceDirect

Metabolic Engineering

journal homepage: www.elsevier.com/locate/meteng





Repurposing plant hormone receptors as chemically-inducible genetic switches for dynamic regulation in yeast

Shuang Wei a , Mengwan Li b , Xuye Lang b,1 , Nicholas R. Robertson b , Sang-Youl Park c , Sean R. Cutler c,d , Ian Wheeldon b,d,e,*

- ^a Biochemistry and Molecular Biology, University of California, Riverside, Riverside, CA, USA
- ^b Chemical and Environmental Engineering, University of California, Riverside, Riverside, CA, USA
- ² Botany and Plant Sciences, University of California, Riverside, Riverside, CA, USA
- ^d Institute for Integrative Genome Biology, University of California, Riverside, Riverside, CA, USA
- e Center for Industrial Biotechnology, University of California, Riverside, Riverside, CA, USA

ABSTRACT

Precise control of gene expression is critical for optimizing cellular metabolism and improving the production of valuable biochemicals. However, hard-wired approaches to pathway engineering, such as optimizing promoters, can take time and effort. Moreover, limited tools exist for controlling gene regulation in non-conventional hosts. Here, we develop a two-channel chemically-regulated gene expression system for the multi-stress tolerant yeast *Kluyveromyces marxianus* and use it to tune ethyl acetate production, a native metabolite produced at high titers in this yeast. To achieve this, we repurposed the plant hormone sensing modules (PYR1^{ABA}/HAB1 and PYR1*MANDI/HAB1*) for high dynamic-range gene activation and repression controlled by either abscisic acid (ABA) or mandipropamid (mandi). To redirect metabolic flux towards ethyl acetate biosynthesis, we simultaneously repress pyruvate dehydrogenase (*PDA1*) and activate pyruvate decarboxylase (*PDC1*) to enhance ethyl acetate titers. Thus, we have developed new tools for chemically tuning gene expression in *K. marxianus* and *S. cerevisiae* that should be deployable across many non-conventional eukaryotic hosts.

1. Introduction

Metabolic engineering seeks to harness native and heterologous pathways for the high titer, rate, and yield production of chemicals. Central to this is the ability to manipulate gene expression. Pathway refactoring using promoters and terminators of known strength, knockout of competing pathways, and overexpression of bottleneck reaction steps are common approaches to enhance the biosynthesis of a desired metabolite. While these approaches are very often successful, they impose static changes on the host cell, which leads to the need for a large set of strains to test multiple conditions. Permanent changes to the genetics of the production host can also be detrimental to cell fitness and prevent the ability to separate growth and product production phases. Dynamic regulation, where gene expression patterns can be altered on cue and at a desired level, can help overcome these challenges, ultimately reducing the number of strains needed for optimization and enabling process strategies that maximize metabolic production, for example, by separating biomass and production phases or by enabling the accumulation of substrate pools before redirecting them to the product pathway.

Starting with the lactose-sensing lac repressor, metaboliteresponsive circuits (e.g., transcriptional regulators, two-component systems, riboswitches, nuclear hormone receptors, and others (Cameron et al., 2014; Kis et al., 2015; McIsaac et al., 2013; Sanford et al., 2022; Wittmann and Suess, 2012)) have been modified to create complex chemically controlled genetic responses in yeast, bacteria, and mammalian cell lines (Arita et al., 2021; Li et al., 2022; Meyer et al., 2019). These systems are robust but provide a limited palette of controlling ligands, many of which are too costly for use in commercial applications or have undesirable pharmacological activity. In yeast, inducible systems that rely on changes in carbon source or media composition (e.g., galactose- and copper-inducible expression (Mascorro-Gallardo et al., 1996; Yocum et al., 1984)) are also widely used, but these systems can introduce physiological changes and are not suitable for use at scale. New regulatory systems controlled by process-friendly ligands would facilitate dynamic regulation in commercial settings.

The plant stress hormone abscisic acid (ABA) is a non-toxic molecule that has been harnessed to engineer ABA-regulated circuits (Jones et al.,

^{*} Corresponding author. Chemical and Environmental Engineering, University of California, Riverside, Riverside, CA, USA. *E-mail address*: wheeldon@ucr.edu (I. Wheeldon).

¹ Current institution: ZJU-Hangzhou Global Scientific and Technological Innovation Center, No.733 Jianshe San Road, Xiaoshan District, Hangzhou, Zhejiang, China, 311,200.

2019; Liang et al., 2011). ABA is perceived by the soluble receptor PYR1 (*Pyrabactin resistance 1*), which forms a stable heterodimer with its coreceptor HAB1 (*Homolog of ABA insensitive 1*) in response to ABA (Park et al., 2009). The PYR1^{ABA}-HAB1 system has several advantages for engineering dynamic regulation. It has a malleable binding pocket that can be mutationally reprogrammed to bind a wide range of chemicals with high affinity, including the low-cost agrochemical mandipropamid, various herbicides, organophosphate pesticides, and natural and synthetic cannabinoids (Beltrán et al., 2022; Park et al., 2015; Zimran et al., 2022). Thus, the PYR1^{ABA} system enables designing processes controlled by user-specified, industry-friendly molecules. A second benefit of this system is a recently developed orthogonal PYR1*MANDI-HAB1* that can operate independently from the wild-type module. The PYR1*MANDI-HAB1* module can also be reprogrammed to bind new ligands and enable multi-input, multi-output genetic circuits (Park et al., 2023).

The PYR1^{ABA}/HAB1 system provides general-purpose modules for constructing dynamic regulatory systems across biological kingdoms; this portability opens new possibilities for metabolic engineering, particularly in non-conventional hosts that lack extensive dynamic regulation systems. Realizing this utility requires developing repressible and inducible systems to control metabolite flux and direct carbon toward desired precursors and products. In this work, we address the need for chemically-regulated gene regulation systems in non-conventional microbial hosts by adapting the PYR1^{ABA}-HAB1 and PYR1*MANDI-HAB1* systems for use in the multi-stress tolerant yeast *Kluyveromyces marxianus*. We demonstrate the utility of these dynamic regulation systems by using them to optimize carbon flux to ethyl acetate (EA), a native *K. marxianus* metabolite with commercial value as a solvent and flavoring agent.

2. Results and discussion

Strains of *K. marxianus* are known to natively produce high levels of EA, an industrial solvent and flavoring agent (Löbs et al., 2016; Löser et al., 2015). In *K. marxianus*, EA synthesis is accomplished by the alcohol acetyltransferase EAT1 (Kruis et al., 2017; Löbs et al., 2018), which condenses ethanol and an acetyl group from acetyl-CoA to produce EA (Fig. 1a). Precursors to this reaction are derived from pyruvate; Pdc1 converts pyruvate to acetaldehyde, which is subsequently converted to ethanol via alcohol dehydrogenase activity, while acetyl-CoA is produced via the pyruvate dehydrogenase complex (Pdh; Pda1 in particular) or via the Acs1/2 conversion of acetate to acetyl-CoA. In a previous study, we demonstrated that repressing the TCA cycle and

down-regulating the electron transport chain redirects carbon flux to ethanol and acetyl-CoA and subsequently to EA by Eat1 activity (Löbs et al., 2018). The CRISPRi repression approach that we took to demonstrate this required a relatively large number of strain engineering steps, the repression conditions were fixed at a single level, and the strategy could only be activated from the outset of the cultures. PYR1-ABA-HAB1 genetic circuits enable a dynamic approach to fine-tune gene expression around the pyruvate node (Fig. 1b). Genetic circuits regulated by low-cost molecules (i.e., ABA and mandipropamid) also enable the separation of biomass production and product formation stages.

PYR1-based chemically regulated activation circuits in Saccharomyces cerevisiae exploit a yeast-two-hybrid approach with multiple split DNA binding and activation domains (DBDs and ADs) fused to PYR1 and HAB1 respectively (Beltrán et al., 2022; Park et al., 2023). Before deploying this system in K. marxianus, we investigated the effects of different circuit architectures and DBDs on circuit function in S. cerevisiae (Fig. S1). We first tested the activation of a report gene (EGFP) with alternative AD-PYR1*MANDI and DBD-HAB1* fusions that swap the architecture and found that all construct designs were functional but that the lowest background and highest fold-change were achieved using the DBD-PYR1*MANDI/AD-HAB1* configuration (here, the AD was VP64 (Jonker et al., 2005) and the DBD was Z4 (McIsaac et al., 2013)). We next explored different DBDs and found that Z4, EP (Weber et al., 2002), LexA (Wade et al., 2005), and ATAF1 (Naseri et al., 2017) fusions to PYR1* were all functional, indicating multiple DBDs can be used (Fig. S2).

Given the success in *S. cerevisiae*, we ported the PYR1*^{MANDI}/HAB1* circuit to *K. marxianus* (Fig. 2a). We first tested to see if ABA or mandi was toxic to *K. marxianus*. No negative growth effects were observed with up to 100 μM of each ligand and 200 μM combined of ABA and mandi (Fig. S3). Reporter gene expression (*EGFP*) was first tested using the synthetic promoter *Z44-ScCYC1*_{core}, but we sought to optimize circuit function by testing a series of *K. marxianus* core promoters (150 bp upstream of the start codon) previously tested in our lab. We found that a synthetic *Z44-HTB1*_{core} promoter (histone B1) achieved the highest fold-change with nM responsiveness to mandipropamid (Fig. 2b and c). The series of tested core promoters ranged in expression level; HTB1 was the strongest of the set (Lang et al., 2020). Of the weaker promoters (SSA3, INU1, PIR1, and PST1) only SSA3 produced a functional circuit, while all medium strength promoters produced at least a 2-fold response in the presence of activating ligand.

To develop a chemically regulated repression system, we tested if a repression domain could substitute for the activation domain in VP64-

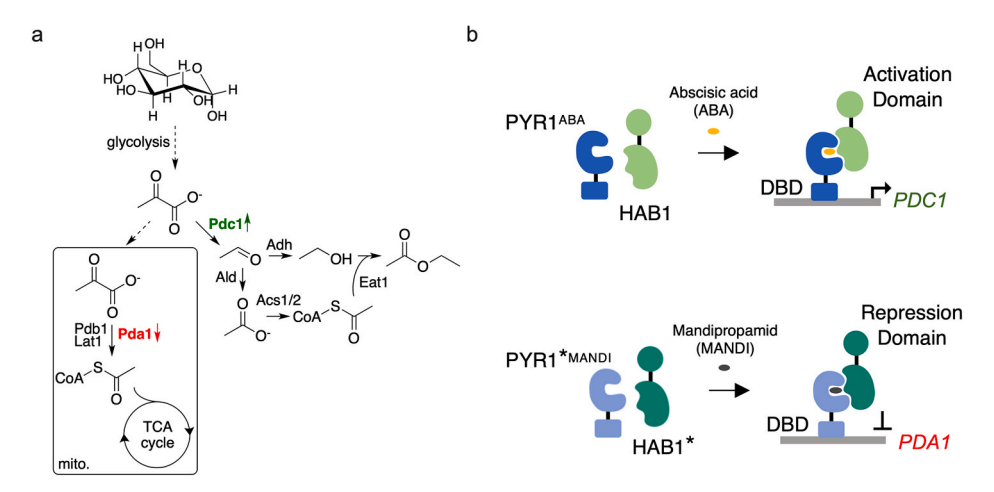


Fig. 1. Dynamic regulation of carbon flux around the pyruvate metabolic node for increased ethyl acetate production in *K. marxianus*. (a) Metabolic pathway for ethyl acetate (EA) biosynthesis in *K. marxianus*. Increased pyruvate flux to acetaldehyde via *PDC1* activation increases ethyl acetate precursor concentrations, while repression of *PDA1*, which is part of the pyruvate dehydrogenase complex, reduces pyruvate flux to the TCA cycle. (b) PYR1-based genetic switches for gene activation and repression. The PYR1^{ABA}-HAB1 chemical-induced dimerization module responsive to the plant hormone ABA activates *PDC1* expression. The PYR1*MAB1* module responds to the agrochemical mandipropamid (mandi) and operates orthogonally to PYR1^{ABA}-HAB1 to repress *PDA1* expression.

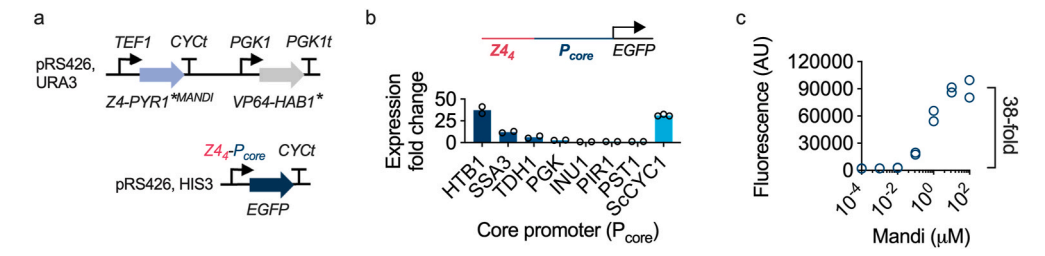


Fig. 2. PYR1-based gene activation in *K. marxianus*. (a) Genetic circuit design of the PYR1*MANDI/HAB1* activation system and reporter gene in *K. marxianus*. The genetic circuit and reporter gene were separately expressed from low copy plasmids, pKmCEN/ARS (Löbs et al., 2017) with *URA3* or *HIS3* auxotrophic markers (here indicated as p*Km*). Four *Z4* DNA binding sequence repeats (*Z4*₄) act as an upstream activating sequence (UAS) for the reporter gene core promoter. (b) Fold change in EGFP fluorescence from various core promoters (P_{core}) when activated with 100 μM mandi. Fluorescence from each condition was measured by flow cytometry. Bars represent the mean, and data points for each replicate are shown. Core promoters are *K. marxianus* sequences except for *ScCYC1*, which is native to *S. cerevisiae*. (c) Response function with the *HTB1* core promoter with mandi concentration ranging from 0.1 nM to 100 μM. Data from two biological replicates is shown. Fluorescence measurements were taken 12 h after induction with the relevant mandi concentration, 30 °C, 990 rpm plate shaking. Activating ligand was added at the outset of the culture.

HAB1*. Six well-characterized *S. cerevisiae* repressors were tested for activity in *K. marxianus* (*TUP1*, *HDT1*, *RPD*, *MBD2B*, *ACR1*, and *HST* (Boeke et al., 2000; Lee and Ziff, 1999; Rusché and Rine, 2001; Varanasi et al., 1996; Vincent and Struhl, 1992)) in combination with *Z4* binding sites placed at variable positions upstream of a *TEF3 K. marxianus* promoter driving expression of a plasmid-localized *EGFP* reporter gene. These experiments determined that positioning four repeats of the *Z4* binding sequence at -150 bp from the start codon combined with TUP1-HAB1* yielded maximal ligand-mediated reductions in *EGFP* expression (Fig. 3a and b). Placing the binding sequence further

upstream decreased the repression effect; expression was increased in the presence and absence of mandi and fold change in expression decreased from a high at -150 bp to less than 2-fold at -400 bp (Fig. S4). This distance-dependent trend has been observed in other transcriptional repression approaches, including CRISPR interference strategies in yeast, which is enhanced with dCas9 binding close to the transcriptional start sites (Löbs et al., 2018; Schwartz et al., 2017a).

Given the success of the *HTB1* promoter for activation, we next sought to test the optimal repression architecture (-150 Z4 $_4$ + TUP1-HAB1 * + Z4-PYR1 * MANDI) with this promoter and found that the

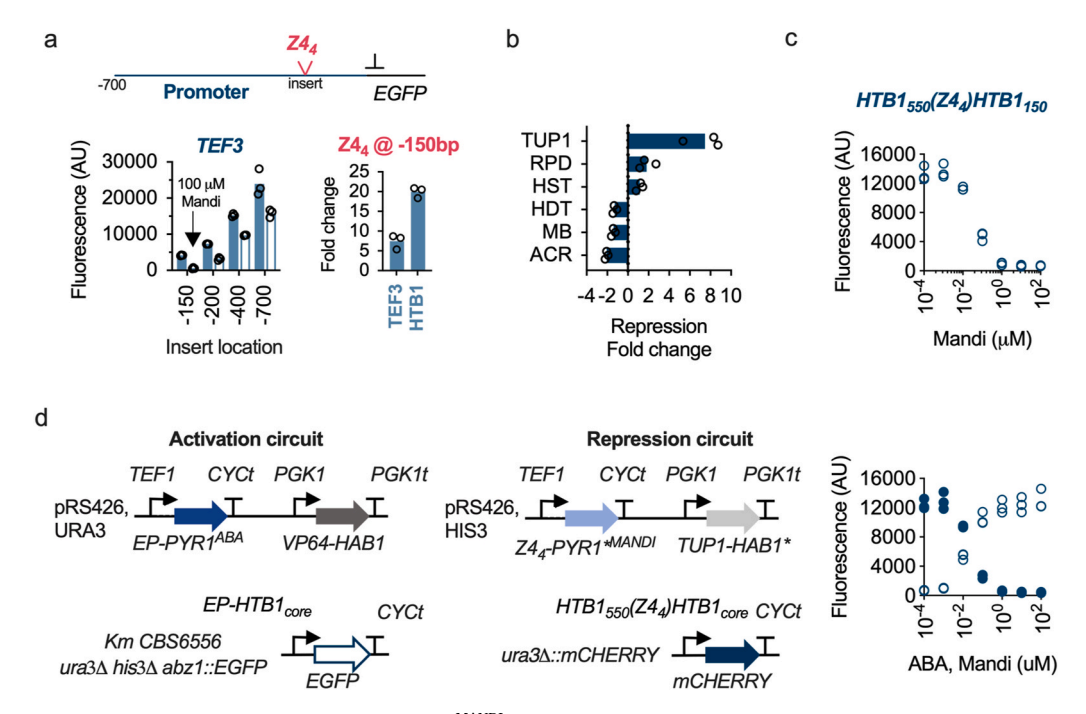


Fig. 3. PYR1-based gene repression in *K. marxianus*. (a) A Z4-PYR1*MANDI/TUP1-HAB1* system was used to repress the expression of *EGFP*. Four repeats of the *Z4* DNA binding sequence ($Z4_4$) were inserted at various locations into the *TEF3* promoter; fluorescence was measured in the presence and absence of mandi (0 μM, solid blue bars; 100 μM open blue bars). The optimal insertion location (-150 bp from the start codon) was tested in *TEF3* and *HTB1* promoters. (b) A series of repression domains were tested using the PYR1*MANDI/HAB1* repression system with a *TEF3* promoter modified with the Z4₄ binding sequence at -150 bp driving the expression of *EGFP*. (c) *EGFP* expression with the optimal repression circuit configuration (Z4-PYR1*MANDI/TUP1-HAB1* + HTB1₅₅₀(Z4₄)HTB_{core}). Data in (a), (b), and (c) were generated with all components expressed from plasmids with a pKmCEN/ARS backbone (see Table S2). PYR1*MANDI/HAB1* were expressed from one plasmid, while the reporter gene was expressed from a separate plasmid, each with a unique auxotrophic marker. (d) Simultaneous activation and repression in *K. marxianus*. The genetic circuit design of the PYR1*MAB1 activation circuit and PYR1*MANDI/HAB1* repression circuit with fluorescent protein reporter genes. The PYR1*MANDI/HAB1 and PYR1*MANDI/HAB1* components were expressed from plasmids, each with a different auxotrophic marker as indicated. The reporter genes were expressed from expression cassettes integrated into the genome of *K. marxianus* CBS6556. The addition of ABA activated *EGFP* expression and the addition of mandi repressed *mCHERRY* expression; both circuits respond with nM sensitivity. Fluorescence measurements were taken 12 h after induction with the relevant ligand concentration. Both ligands were added to cultures grown at 30 °C, 990 rpm plate shaking. Fluorescence from each condition was measured by flow cytometry. Bars represent the mean, and data points for each replicate are shown (n = 3).

repression fold change was enhanced; maximal repression with HTB1 yielded a 22-fold reduction in EGFP expression at saturating ligand concentrations with a low nanomolar EC_{50} (Fig. 3c).

With an optimized repression system in hand, we next set out to test whether gene activation and repression could function simultaneously. To do so, we integrated *EGFP* and *mCHERRY* reporter genes into genomic landing sites (Li et al., 2021) and expressed an ABA-responsive PYR1-activation circuit and a mandi-responsive PYR1*-repression circuit from separate plasmids (Fig. 3d). The circuits functioned as expected, activating *EGFP* expression and repressing *mCHERRY* expression by 19- and 32-fold, respectively.

The tandem PYR1-based activation and repression systems provide an opportunity for the dynamic control of chemical biosynthesis in K. marxianus. Known for its high native capacity to produce EA, we sought to test this ability to redirect carbon flux to EA precursors in K. marxianus. To do this, we replaced the native promoter of PDC1 with (EP₄)HTB1_{core}, which is activated by EP-PYR1^{ABA}/VP64-HAB1 upon the addition of ABA. We also replaced the native PDA1 promoter with HTB1₅₅₀(Z4₄)HTB1_{core} for repression with mandi (Fig. 4a) to create a K. marxianus strain (called dynKm) for dynamic control of gene expression. A chemical refactoring experiment using three levels of induction and repression revealed that the expression level of both genes could be effectively modulated with up to 21-fold activation of PDC1 and 17-fold repression of PDA1 (Fig. S5). This experiment tested ABA and mandi inducer levels corresponding to low, intermediate, and high expression or repression by adding 0, 1, and 10 μM of ABA and mandi. Given the essential role that Pda1 plays in aerobic metabolism, we anticipated that substantial repression of this gene would limit cell growth. This proved true, as PDA1 repression with 1 and 10 µM mandi resulted in cultures with cell densities, almost half that achieved with no or low repression (Fig. S6). Given this, we limited the repression of PDA1 in EA optimization experiments to 1 μM or less while using the full range of ABA-induced activation of PDC1.

The 3-level refactoring experiment with the reduced repression range for *PDA1* revealed that EA biosynthesis was significantly enhanced with partial *PDA1* repression and full activation of *PDC1* (Fig. 4b). This condition, however, also resulted in increased ethanol over the unregulated condition, indicating an imbalance in EA precursors. Given this, we sought to explore a finer range of transcriptional conditions. Using the activation and repression circuit response curves as a guide, we estimated the ligand concentrations necessary to create a series of conditions that increase by $\sim\!10\%$ activation or repression at each step. With the addition of 5.36 μM ABA and the addition of 0.35 μM mandi, EA biosynthesis was increased to more than 132 mg L $^{-1}$ OD $^{-1}$ (Fig. 4c), a 4.4-fold increase over the baseline strain in the absence of ABA and mandi-induced gene regulation.

Our dynamic regulation strategy seeks to redirect pyruvate flux away from the TCA cycle and toward acetaldehyde via Pdc1 activity. We hypothesize that this strategy will increase ethanol biosynthesis and balance EA precursors to maximum production; however, there is the possibility that this strategy will instead lead to an increase in the acetyl-CoA pool as acetaldehyde can be converted to acetate and subsequently to acetyl-CoA via acetyl-CoA synthetase activity encoded by ACS1 and ACS2 (Sakihama et al., 2019). To test this, we created single knockouts of ACS1 and ACS2 in the dynKm strain and subjected the mutant strains to the 3-level chemical refactoring experiment (Fig. 5a). These optimization experiments yielded results similar to those conducted with functional ACS1 and ACS2; EA production was maximized with full PDC1 activation and partial repression of PDA1. This suggests that our initial hypothesis was correct - redirecting pyruvate flux to acetaldehyde leads to increased ethanol production and, consequently, increased EA. Disrupting ACS1 and ACS2 likely reduced the available acetyl-CoA pool as total EA production from these strains was reduced compared to dynKm with functional acetyl-CoA synthase activity (Fig. 5b).

With optimized induction and repression levels in hand, we next sought to test the timing of the dynamic regulation strategy. EA exhibits

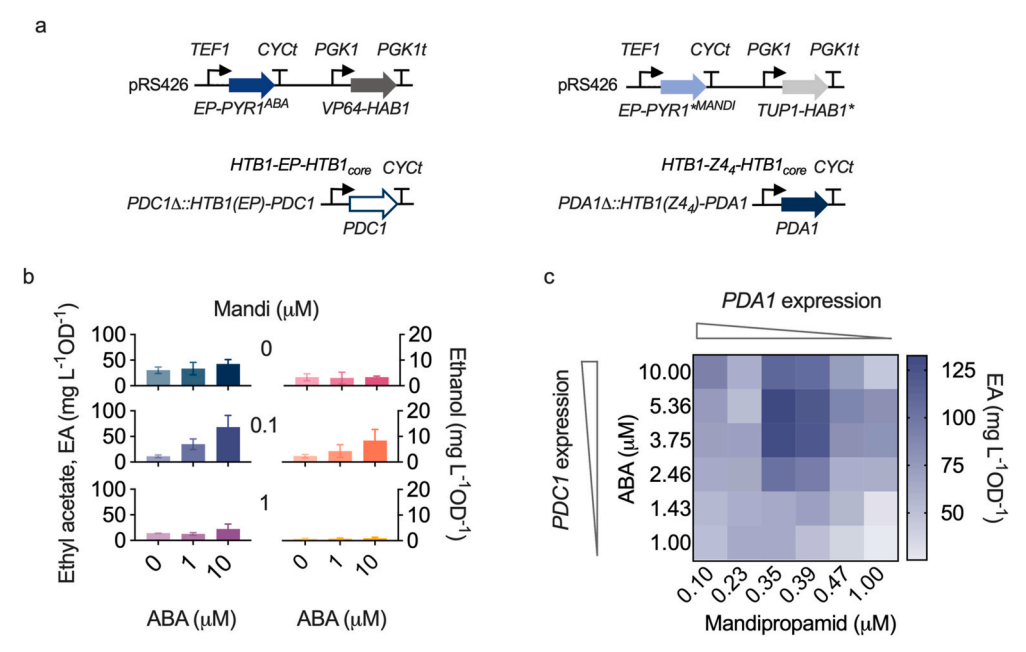
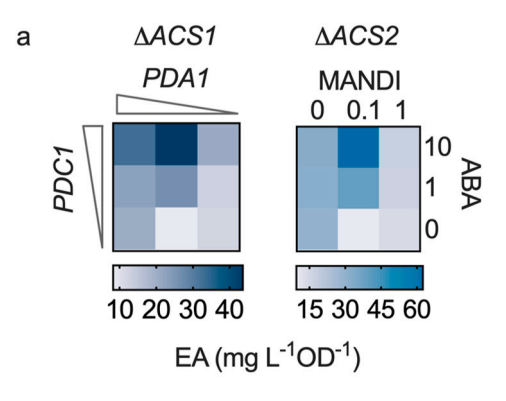


Fig. 4. Chemical control of pyruvate flux to ethyl acetate precursors and increases ethyl acetate biosynthesis. (a) Genetic circuit design for the activation of *PDC1* and repression of *PDA1* in the *K. marxianus* CBS6556 strain dynKm. PYR1^{ABA} and PYR1*^{MANDI}-based genetic switches were expressed from CEN/ARS low-copy plasmids (pKm). The native promoters for *PDC1* and *PDA1* were replaced with synthetic *HTB1* promoters with *EP* upstream activation (*PDC1*) and *Z4* upstream repression sequences (*PDA1*) based on designs optimized in Figs. 2 and 3. (b) Specific titer of ethyl acetate (EA; left) and ethanol (right) in g L¹ OD⁻¹ with combinations of ABA-induced activation of *PDC1* and mandi induced repression of *PDA1*. ABA induction concentrations are shown on the x-axis, while the concentration of mandi for each set of ABA inductions is indicated for each pair of EA and ethanol measurements. (c) Optimization of ABA and mandi induction conditions to maximize EA biosynthesis. The heat map shows EA-specific titer with ABA ranging from 1 to 10 μM and mandi from 0.1 to 1 μM. Metabolite measurements (b and c) were acquired after 20 h of cultivation at 30 °C in a 25 mL SD-U-H medium, 300 rpm shaking. All experiments were performed in biological triplicate. Bars represent the mean, while error bars represent the standard deviation. The heat map color scale indicates specific EA titers in mg L⁻¹ OD⁻¹.



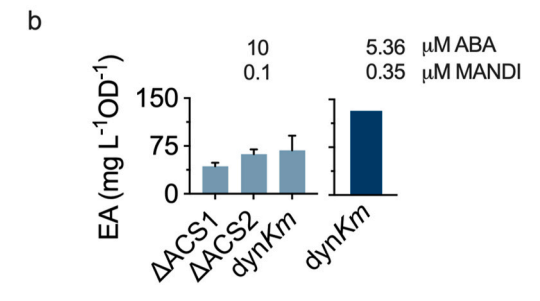


Fig. 5. Pyruvate flux optimization is not affected by acetyl-CoA activity. (a) Optimization of ABA and mandi induction conditions to maximize EA biosynthesis without acetyl-CoA synthetase activity. The heat maps show EA-specific titer with ABA ranging from 1 to 10 μ M and mandi from 0.1 to 1 μ M with K. marxianus CBS 6556 PDC1 Δ ::EP4-HTB1-PDC1 PDA1 Δ ::HTB1-Z44-PDA1 ura3 Δ his3 Δ (indicated here as dynKm). The left-hand heat map was generated with ACS1 disrupted; the right-hand map with ACS2 disrupted. (b) Comparison of EA-specific titers achieved with and without functional ACS1 and ACS2 and induction conditions from the coarse and fine grain chemical refactoring experiments. Metabolite measurements were acquired after 20 h of cultivation at 30 °C in a 25 mL SD-U-H medium with 300 rpm shaking. All experiments were performed in biological triplicate. Bars represent the mean, while error bars represent the standard deviation. The heat map color scale indicates specific EA titers in mg L $^{-1}$ OD $^{-1}$.

a growth-dependent production profile (Löbs et al., 2017); we manipulated PDC1/PDA1 expression during early exponential growth so cellular resources would be directed toward EA biosynthesis when growth rates are maximal. Activation and repression of PDC1 and PDA1 in the early exponential phase (12 h post-inoculation) increased EA biosynthesis to $151 \text{ mg L}^{-1} \text{ OD}^{-1}$. EA titers were 33% higher than when ABA and mandi were added at the outset of the culture and 55% higher than the uninduced condition (Fig. 6). While EA production was higher with dynamic pyruvate metabolism initiated during the exponential phase, glucose consumption and EA production profile were generally consistent; glucose consumption approached completion at 24 h, and EA titers reached a maximum between 20 and 22 h post-inoculation. In addition, ethanol production was low in all cases. We note that ethyl acetate production from the wild type strain of *K. marxianus* CBS6556 is on par with our optimized dynamic regulation strategy (Löbs et al., 2017), suggesting that further strain engineering (e.g., integration of the sensor system) is still needed prior to deploying this strategy in bioprocesses.

Regulated transcription systems are core technological tools for dynamically tuning regulatory network nodes. Our work demonstrates chemically-mediated activation and repression of target genes using simple, low-cost inducers with the PYR1^{ABA}/HAB1 and PYR1*^{MANDI}/HAB1* dimerization systems. Although several systems for regulated transcription have been developed in *S. cerevisiae*, including the PYR1/HAB1 system, relatively few have been developed for and validated in non-conventional yeasts, such as *K. marxianus*. We see several advantages that our system offers for metabolic engineering. First, the PYR1/

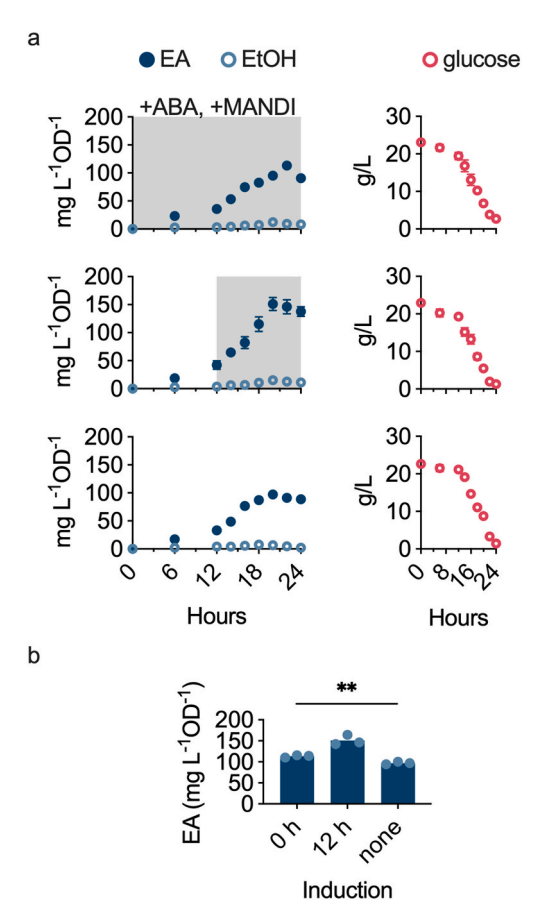


Fig. 6. Time-dependent dynamic regulation of EA biosynthesis in *K. marxianus*. (a) Time-course of specific EA and ethanol titers and consumption of glucose for various dynamic regulation strategies, including activation of *PDC1* and repression of *PDA1* upon inoculation (t=0 h), at the outset of exponential phase (t=12 h), and no induction (top, middle, bottom, respectively). Data points represent the mean, while error bars represent the standard deviation. In some cases, error bars are within the data points and are therefore not shown. Growth data provided in Supporting Figure S7. (b) Comparison of maximum specific EA titer. Maximum specific titers were achieved between 20 and 22 h. All experiments were performed in biological triplicate: 30 °C in 25 mL SD-U-H medium, 300 rpm shaking. Data points are shown for each replicate; bars represent the mean.

HAB1 scaffolds provide new expression systems controlled by low-cost chemicals (ABA, mandi, and others (Beltrán et al., 2022; Park et al., 2023)) that are suitable for use at scale. Both ABA and mandipropamid are used in industrial agriculture: ABA is used as a fruit ripening agent and as a means to induce drought tolerance; mandipropamid is a fungicide often used on vegetable crops to defend against downy mildew and Phytophthora blight. These at scale uses provide evidence for their potential for use in industrial microbial bioprocesses. Second, our work provides tools for facile chemical tuning of metabolic nodes, empowering efforts to harness and manipulate the immense biochemical diversity afforded by non-conventional yeasts. The tools created here leverage our experience in optimizing PYR1 and PYR1* sensor systems for use in S. cerevisiae and in the plant species Arabidopsis thaliana (Beltrán et al., 2022; Park et al., 2023). Adopting these platforms for use in K. marxianus required the design of new expression constructs that use species specific promoters, thus providing an example of how these systems can be adopted for use in other non-conventional yeast and industrially relevant eukaryotic metabolic engineering hosts. Third, our systems enable chemical refactoring experiments, which reduce the number of strains needed for optimization and accelerate the exploration of biochemical solution space. Creating new strains, particularly in non-conventional species, is a bottleneck in our engineering pipelines that can take weeks. Taken together, the advantages, beneficial characteristics, and portability with respect to host species, of the PYR1 system makes for a promising platform for engineering dynamic regulation in a broad range of metabolic engineering hosts.

3. Conclusion

We have tackled the challenge of dynamic gene regulation in the yeast *K. marxianus*, aiming to enhance the production of ethyl acetate, a naturally occurring metabolite of significant commercial interest. We developed a two-channel, chemically-regulated gene expression system that leverages plant-derived PYR1^{ABA}/HAB1 and PYR1*MANDI/HAB1* hormone-sensing modules to engineer induction and repression circuits. We optimized the architectures of these modules and then used them to control the activity of key EA nodes (*PDC1* and *PDA1*). This approach allowed us to redirect metabolite flux and improve ethyl acetate titers. Our ABA and mandipropamid-controlled dual-channel systems function in both *K. marxianus* and *S. cerevisiae* and should function widely across eukaryotic hosts, given our use of standard biological parts. Our approach illustrates how dynamic control of gene expression facilitates metabolic engineering using non-toxic and low-cost molecules deployable at scale.

4. Materials and methods

4.1. Strains, plasmids, and cell culture

All yeast strains and plasmids used in this work are listed in Tables S1 and S2. Notably, S. cerevisiae strain BY4742 ura3Δ his3Δ LeuΔ TrpΔ was utilized as the base S. cerevisiae strain, while K. marxianus strain CBS 6556 ura3∆ his3∆ was used as the base K. marxianus strain. Strains without plasmids were grown in YPD media (10 g L⁻¹ yeast extract, 5 g L⁻¹ peptone; DB Difco®, Becton-Dickinson, 20 g L⁻¹ glucose). All yeast strains harboring plasmids with auxotrophic markers were cultured with synthetic defined (SD) media minus the selective amino acid. For example, strains containing plasmids with a uracil auxotrophic marker were cultured in SD-U media: 6.7 g L⁻¹ BD Difco™ Yeast Nitrogen Base without amino acids (Sigma-Aldrich), 1.92 g L⁻¹ Yeast Synthetic Dropout Medium Supplements without uracil (Sunrise Science Products), and 20 g L⁻¹ D-glucose. K. marxianus and S. cerevisiae strains were grown at 30 °C. Liquid cell cultures in shake flasks were grown at 300 rpm in a shaker incubator. Liquid cell cultures in 96 deep-well plate format were grown at 990 rpm in a shaker incubator.

4.2. Yeast transformation

For *K. marxianus*, a single colony was picked and grown in 2 mL YPD for 16 h at 30 °C. One milliliter of cell culture was harvested by centrifugation at 5000g for 2 min. The supernatant was removed, and the pellet was washed with an equal volume of sterile ddH_2O . Pelleting and washing were repeated twice before moving forward with the transformation protocol. Washed cell pellets were suspended in 100 µg salmon sperm carrier DNA (R&D SystemsTM Salmon Sperm DNA) and 0.2–1 µg of DNA. Five hundred milliliters of transformation mix containing 40% polyethylene glycol 3350 (Fisher Scientific), 0.1 M lithium acetate, 10 mM Tris-HCl (pH 7.5), 1 mM EDTA disodium salt dihydrate (Sigma-Aldrich) and 10 mM Dithiothreitol (Fisher Scientific), was added. The solution was incubated at room temperature for 15 min and subsequently heat shocked at 48 °C for 15 min. The transformed cells were plated on solid selective media (e.g., SD-U for URA3 markered plasmids).

For *S. cerevisiae*, a single colony was picked and grown to stationary phase in YPD and then diluted to a 1:50 ratio in YPD and grown for 4-6 h. Cells were harvested by centrifugation at 4000g for 10 min. An equal volume of sterile ddH_2O was used to wash cells twice. The cell pellet was

suspended in $100~\mu g$ carrier DNA and $0.2-1~\mu g$ of plasmid or linear DNA. 500~mL of transformation mix, which contains 40% polyethylene glycol 3350,~0.1~M lithium acetate, 10~mM Tris-HCl (pH 7.5), 1~mM EDTA disodium salt dihydrate, and 10~mM dithiothreitol, was added and the solution was incubated at room temperature for 45~min and subsequently heat shocked at $42~^{\circ}C$ for 45~min. The transformed cells were plated on solid SD-U agar plates or the appropriate selective media.

4.3. Molecular cloning and reagents

All primers used in this work are listed in Table S2. All generated gene construct sequences and plasmid maps are provided as Multimedia Compenents 1-38. Cloning reagents and restriction enzymes were purchased from New England Biolabs (NEB). All primers for DNA amplifications were purchased from Integrated DNA Technologies (IDT). The Q5® High-Fidelity DNA polymerase system was used for DNA amplification. NEBuilder® HiFi DNA Assembly Master Mix was used for Gibson assembly. All PCR products and linearized vectors were fractionated by agarose gel electrophoresis and purified using a Zymo Research gel extraction kit. All plasmids were propagated in *E. coli* TOP10 cells (Thermo Fisher Scientific), and plasmid extractions were performed with the Zymo Research plasmid miniprep kit. All g-block DNA fragments used in this work are provided in Table S5.

4.4. Dual K. marxianus reporter strain

A single K. marxianus strain with two fluorescent reporter genes was constructed to investigate simultaneous activation and repression. EGFP was used as a reporter for repression, while mCHERRY was used as a reporter for activation. The activation report expression cassette (HBT1₅₅₀-Z4₄-HTB1_{core}-EGFP-CYC1t) was inserted into the K. marxianus genome at the ABZ1 locus using CRISPR-mediated integration (Li et al., 2021; Schwartz et al., 2017b). The repression reporter cassette (EP4-HTB1core-mCHERRY-CYC1t) was subsequently integrated into this strain using the same procedure. Briefly, a two-plasmid system was used to integrate each gene. One plasmid encodes 700 bp of up- and downstream homology to the integration site ABZ1 locus and the gene to be integrated; a second plasmid expresses CAS9 and cognate sgRNA. Co-transformed cells are outgrown and plated on selective media, with PCR screening to confirm reporter gene integration. K. marxianus strain CBS 6556 abz1::EGFP ura3\Delta his3\Delta was created using pIW1134 and pIW1135. CBS 6556 abz1::EGFP ura3::mCHERRY his3∆ was created using pIW1123 and pIW1124.

4.5. PDA1 and PDC1 dynamic regulation strain

The approach to creating a strain with inducible activation of PDC1 and repression of PDA1 was based on the CRISPR-mediated gene integration strategy described in section 4.4. Briefly, sgRNAs targeting the first 700 bp of each gene's promoter region were designed using CCTop and CRISPRater (https://crispr.cos.uni-heidelberg.de/) (Labuhn et al., 2018; Stemmer et al., 2015). The top predicted sgRNAs were each inserted into a PspXI linearized K. marxianus CRISPR-Cas9 vector, pIW601 by Gibson cloning (see Table S3 for all sgRNAs used in this work). The repair plasmids, one for PDA1 and a second for PDC1, encoded an integration cassette with 700 bp homology to the upstream promoter region (-1400 to -700 bp), and 700 bp homology to the coding sequence beginning at the transcriptional start site (pSW267 and pSW300). The homology donor regions were assembled into SacII and XhoI digested pIW1135. Using sgRNAs targeting PDA1 and a PDA1 repair plasmid, TEF1550-EP4-HTB1core, replaced the native PDA1 promoter. Using sgRNAs targeting PDC1 and a PDC1 repair template, the synthetic promoter Z4₄-HTB1_{core} replaced the native PDC1 promoter. The genotype of K. marxianus CBS 6556 PDA1::Z44-PDA1 PDC1:: EP_4 -PDC1 ura3 Δ his3 Δ was confirmed by Sanger sequencing.

4.6. Chemical refactoring of PDA1 and PDC1 expression

Single colonies were inoculated into 2 mL SD-U-H in a 14-mL culture tube (USA Scientific, Orlando, FL, USA) and grown at 30 $^{\circ}C$, 300 rpm overnight in a Multitron Pro shaker incubator (INFORS HT, Bottmingen, Switzerland). The overnight cultures were diluted 1:500 into 25 mL SD-U-H and grown at 30 $^{\circ}C$, 300 rpm. Ethyl acetate production was first measured after culturing in all combinations of mandipropamid (0, 0.1, and 1 μ M) and ABA (0, 1, and 10 μ M). The next search was performed by dividing the concentration range with higher ethyl acetate production into 6 groups. All combinations of 0.1, 0.23, 0.35, 0.39, 0.47, 1 μ M mandipropamid, 1, 1.43, 2.46, 3.74, 5.36,10 μ M ABA were tested.

4.7. Construction of PYR1-based activation and repression circuits

All PYR1-based genetic circuits were built using previously described parts validated in *S. cerevisiae* (Beltrán et al., 2022; Park et al., 2023). Briefly, PYR1^{ABA}/HAB1 and PYR1*MANDI/HAB1* expression cassettes were amplified from previously described constructs and assembled using a combination of Gibson assembly and conventional cloning into *K. marxianus* expression vectors (pRS426 backbone). The tested repression domains that enabled a repression circuit (*TUP1*, *HDT1*, *RPD*, *MBD2B*, *ACR1*, *HST*, and *MXI1*) were amplified from *S. cerevisiae* genomic material and cloned into the HAB1* expression cassette after digestion with Eag 1/Ale 1. Upstream repressing positions (-150, -200, -400, and -700 bp from the translational start site) were selected based on core promoter design (150 bp) and increasing distances upstream, exploring up to 700 bp from the start site. All plasmid sequences are provided in Multimedia Components 2-38.

4.8. Flow cytometry analysis of cellular fluorescence

Three single transformants were used to inoculate 2 mL SD-U media cultures containing 2% glucose and pre-cultured; cells were then passaged into wells of a 96-deep-well plate (USA Scientific, Orlando, FL, USA) in 1 mL media (OD₆₀₀ = 0.1). Up to 5 μ L of ligand stocks (solvated in DMSO) were added immediately after inoculation, plates sealed with an AeraSeal film (Excel Scientific, Victorville, CA, USA), and grown at 990 rpm, and 90 % humidity for 12 h. The cells were harvested by centrifuge at 5000 g for 10 min. After discarding the supernatant, the cells were suspended in 1 mL phosphate-buffered saline (PBS) (Sigma Aldrich) and centrifuged at 5000 g for 10 min. The cells were washed twice with 1 mL PBS and suspended in 1 mL DI water for flow cytomety analysis. BD accuriTM C6 flow cytometer (BD Bioscience) was used for data collection and analysis. A control cell population without fluorescent protein expression was first run to identify basal cell autofluorescence before collecting data for the experimental samples. For each sample, 10,000 events were collected. The forward scatter, side scatter, EGFP fluorescence, and mCHERRY fluorescence were recorded for each event. All experiments were performed in biological triplicate.

4.9. Metabolite quantification

Ethyl acetate (EA) was extracted from culture media with cyclohexane (ReagentPlus., \geq 99%; Sigma Aldrich) and quantified by gas chromatography. Extraction began with collecting 700 µL media from 24-h cell cultures centrifuged at 5000 g for 10 min 500 µL of the media was transferred to another tube to which an equal volume of solvent was added. The two-phase solution was vortexed for 30 min, and 100 µL of the cyclohexane layer was collected after centrifugation at 10,000 g for 1 min. Quantification was performed with a Shimadzu GC-2010 Plus equipped with a Shimadzu AOC-20s autosampler, AOC-20i autoinjector, and FID detector. An Agilent J&W DB-WAX Ultra Inert column (length: 30 m; inner diameter: 0.32 mm; film thickness: 0.5 µm) was used for separations. One microliter samples were injected and subjected to a temperature ramp starting at 100 °C, increasing to 140 °C at

 $20\,^{\circ}\text{C/min}$, then increasing to $150\,^{\circ}\text{C}$ at $10\,^{\circ}\text{C/min}$, holding at $160\,^{\circ}\text{C}$ for $2\,$ min after at $5\,^{\circ}\text{C/min}$ increase, holding again from $2\,$ min at $170\,^{\circ}\text{C}$ after increasing at $1\,^{\circ}\text{C/min}$, and finally, increasing to $220\,^{\circ}\text{C}$ at $25\,^{\circ}\text{C/min}$. Helium was used as a carrier gas at a flow rate of $1.9\,$ mL/min. Using these methods, the retention time of EA was determined to be $3.9\,$ min. EA quantification was aided by standard curves linking the FID peak area of EA extracted from SD-H-U media containing $1,\,2,\,4,\,20,\,$ and $100\,$ mg L $^{-1}$ EA subjected to the extraction protocol described above.

Extracellular glucose and ethanol were quantified by HPLC analysis. Briefly, 1 mL of spent media was collected from cell culture samples centrifuged at 5000 g for 10 min. The supernatant was filtered through a 0.2 μm filter (VWD) and analyzed using an Aminex HPX-87H column (Bio-rad) in an Ultimate 2200 HPLC system (ThermoFisher Scientific). Eluting with 0.8 L min $^{-1}$ of 5 mM $\rm H_2SO_4$ at 60 °C, glucose had a retention time of 3.7 min while ethanol eluted at 7.1 min. Calibration curves for both compounds were created using a series of SD-H-U solutions with 10, 50, 100, 200, and 500 mg L $^{-1}$ of glucose and ethanol and analyzed as described above.

4.10. Reverse transcription quantitative PCR (RT-qPCR)

Total RNA from each strain was extracted using the YeaStar™ RNA Kit (Zymo Research). RNA was treated with DNAse (DNAse I, New-England Biolabs) for 10 min and subsequently extracted using the RNA Clean & Concentrator™-5 Kit (Zymo Research). cDNA was obtained using theiScript™ Reverse Transcription Supermix for RT-qPCR (Bio-Rad). SYBR Green qPCR (SsoAdvanced™ Universal SYBR; Green Supermix, Bio-Rad) was used for quantification using a Bio-Rad CFX Connect™ Real-Time PCR Detection System. All primers are provided in Table S4. Chemically induced expression levels were compared using transcript levels normalized to GAPDH.

CRediT authorship contribution statement

Shuang Wei: Writing – review & editing, Writing – original draft, Visualization, Validation, Methodology, Investigation, Formal analysis. Mengwan Li: Writing – review & editing, Methodology, Investigation. Xuye Lang: Writing – review & editing, Methodology, Investigation. Nicholas R. Robertson: Writing – review & editing, Writing – original draft, Visualization, Validation. Sang-Youl Park: Resources, Methodology. Sean R. Cutler: Writing – review & editing, Writing – original draft, Supervision, Conceptualization. Ian Wheeldon: Writing – review & editing, Writing – original draft, Visualization, Supervision, Project administration, Methodology, Funding acquisition, Formal analysis, Conceptualization.

Data availability

Data will be made available on request.

Acknowledgments

This work was supported by Defense Advanced Research Projects Agency Advanced Plant Technologies (DARPA-APT, HR001118C0137), DOE DE-SC0019093, NSF-1803630, NSF-2128016, and NSF-1922642. The views, opinions, and/or findings expressed are those of the authors and should not be interpreted as representing the official views or policies of the Department of Defense or the U.S. Government. Approved for Public Release, Distribution Unlimited.

Appendix A. Supplementary data

Supplementary data to this article can be found online at https://doi. org/10.1016/j.ymben.2024.03.006.

References

- Arita, Y., Kim, G., Li, Z., Friesen, H., Turco, G., Wang, R.Y., Climie, D., Usaj, M., Hotz, M., Stoops, E.H., Baryshnikova, A., Boone, C., Botstein, D., Andrews, B.J., McIsaac, R.S., 2021. A genome-scale yeast library with inducible expression of individual genes. Mol. Syst. Biol. 17. e10207.
- Beltrán, J., Steiner, P.J., Bedewitz, M., Wei, S., Peterson, F.C., Li, Z., Hughes, B.E., Hartley, Z., Robertson, N.R., Medina-Cucurella, A.V., Baumer, Z.T., Leonard, A.C., Park, S.-Y., Volkman, B.F., Nusinow, D.A., Zhong, W., Wheeldon, I., Cutler, S.R., Whitehead, T.A., 2022. Rapid biosensor development using plant hormone receptors as reprogrammable scaffolds. Nat. Biotechnol. 40, 1855–1861.
- Boeke, J., Ammerpohl, O., Kegel, S., Moehren, U., Renkawitz, R., 2000. The minimal repression domain of MBD2b overlaps with the methyl-CpG-binding domain and binds directly to Sin3A. J. Biol. Chem. 275, 34963–34967.
- Cameron, D.E., Bashor, C.J., Collins, J.J., 2014. A brief history of synthetic biology. Nat. Rev. Microbiol. 12, 381–390.
- Jones, K.A., Kentala, K., Beck, M.W., An, W., Lippert, A.R., Lewis, J.C., Dickinson, B.C., 2019. Development of a split esterase for protein-protein interaction-dependent small-molecule activation. ACS Cent. Sci. 5, 1768–1776.
- Jonker, H.R.A., Wechselberger, R.W., Boelens, R., Folkers, G.E., Kaptein, R., 2005. Structural properties of the promiscuous VP16 activation domain. Biochemistry 44, 827–839.
- Kis, Z., Pereira, H.S., Homma, T., Pedrigi, R.M., Krams, R., 2015. Mammalian synthetic biology: emerging medical applications. J. R. Soc. Interface 12. https://doi.org/ 10.1098/rsif.2014.1000.
- Kruis, A.J., Levisson, M., Mars, A.E., van der Ploeg, M., Garcés Daza, F., Ellena, V., Kengen, S.W.M., van der Oost, J., Weusthuis, R.A., 2017. Ethyl acetate production by the elusive alcohol acetyltransferase from yeast. Metab. Eng. 41, 92–101.
- Labuhn, M., Adams, F.F., Ng, M., Knoess, S., Schambach, A., Charpentier, E.M., Schwarzer, A., Mateo, J.L., Klusmann, J.-H., Heckl, D., 2018. Refined sgRNA efficacy prediction improves large- and small-scale CRISPR-Cas9 applications. Nucleic Acids Res. 46, 1375–1385.
- Lang, X., Besada-Lombana, P.B., Li, M., Da Silva, N.A., Wheeldon, I., 2020. Developing a broad-range promoter set for metabolic engineering in the thermotolerant yeast. Metab Eng Commun 11, e00145.
- Lee, T.C., Ziff, E.B., 1999. Mxi1 is a repressor of the c-Myc promoter and reverses activation by USF. J. Biol. Chem. 274, 595–606.
- Liang, F.-S., Ho, W.Q., Crabtree, G.R., 2011. Engineering the ABA plant stress pathway for regulation of induced proximity. Sci. Signal. 4, rs2.
- Li, H.-S., Israni, D.V., Gagnon, K.A., Gan, K.A., Raymond, M.H., Sander, J.D., Roybal, K. T., Joung, J.K., Wong, W.W., Khalil, A.S., 2022. Multidimensional control of therapeutic human cell function with synthetic gene circuits. Science 378, 1227–1234.
- Li, M., Lang, X., Moran Cabrera, M., De Keyser, S., Sun, X., Da Silva, N., Wheeldon, I., 2021. CRISPR-mediated multigene integration enables Shikimate pathway refactoring for enhanced 2-phenylethanol biosynthesis in Kluyveromyces marxianus. Biotechnol. Biofuels 14, 3.
- Löbs, A.-K., Engel, R., Schwartz, C., Flores, A., Wheeldon, I., 2017. CRISPR-Cas9-enabled genetic disruptions for understanding ethanol and ethyl acetate biosynthesis in. Biotechnol. Biofuels 10, 164.
- Löbs, A.-K., Lin, J.-L., Cook, M., Wheeldon, I., 2016. High throughput, colorimetric screening of microbial ester biosynthesis reveals high ethyl acetate production from Kluyveromyces marxianus on C5, C6, and C12 carbon sources. Biotechnol. J. 11, 1274–1281.
- Löbs, A.-K., Schwartz, C., Thorwall, S., Wheeldon, I., 2018. Highly multiplexed CRISPRi repression of respiratory functions enhances mitochondrial localized ethyl acetate biosynthesis in Kluyveromyces marxianus. ACS Synth. Biol. 7, 2647–2655.
- Löser, C., Urit, T., Keil, P., Bley, T., 2015. Studies on the mechanism of synthesis of ethyl acetate in Kluyveromyces marxianus DSM 5422. Appl. Microbiol. Biotechnol. 99, 1131–1144.

- Mascorro-Gallardo, J.O., Covarrubias, A.A., Gaxiola, R., 1996. Construction of a CUP1 promoter-based vector to modulate gene expression in Saccharomyces cerevisiae. Gene 172, 169–170.
- McIsaac, R.S., Oakes, B.L., Wang, X., Dummit, K.A., Botstein, D., Noyes, M.B., 2013. Synthetic gene expression perturbation systems with rapid, tunable, single-gene specificity in yeast. Nucleic Acids Res. 41, e57.
- Meyer, A.J., Segall-Shapiro, T.H., Glassey, E., Zhang, J., Voigt, C.A., 2019. Escherichia coli "Marionette" strains with 12 highly optimized small-molecule sensors. Nat. Chem. Biol. 15, 196–204.
- Naseri, G., Balazadeh, S., Machens, F., Kamranfar, I., Messerschmidt, K., Mueller-Roeber, B., 2017. Plant-derived transcription factors for orthologous regulation of gene expression in the yeast Saccharomyces cerevisiae. ACS Synth. Biol. 6, 1742–1756.
- Park, S.-Y., Fung, P., Nishimura, N., Jensen, D.R., Fujii, H., Zhao, Y., Lumba, S., Santiago, J., Rodrigues, A., Chow, T.-F.F., Alfred, S.E., Bonetta, D., Finkelstein, R., Provart, N.J., Desveaux, D., Rodriguez, P.L., McCourt, P., Zhu, J.-K., Schroeder, J.I., Volkman, B.F., Cutler, S.R., 2009. Abscisic acid inhibits type 2C protein phosphatases via the PYR/PYL family of START proteins. Science 324, 1068–1071.
- Park, S.-Y., Peterson, F.C., Mosquna, A., Yao, J., Volkman, B.F., Cutler, S.R., 2015. Agrochemical control of plant water use using engineered abscisic acid receptors. Nature 520, 545–548.
- Park, S.-Y., Qiu, J., Wei, S., Peterson, F.C., Beltrán, J., Medina-Cucurella, A.V., Vaidya, A. S., Xing, Z., Volkman, B.F., Nusinow, D.A., Whitehead, T.A., Wheeldon, I., Cutler, S. R., 2023. An orthogonalized PYR1-based CID module with reprogrammable ligand-binding specificity. Nat. Chem. Biol. https://doi.org/10.1038/s41589-023-01447-7.
- Rusché, L.N., Rine, J., 2001. Conversion of a gene-specific repressor to a regional silencer. Genes Dev. 15, 955–967.
- Sakihama, Y., Hidese, R., Hasunuma, T., Kondo, A., 2019. Increased flux in acetyl-CoA synthetic pathway and TCA cycle of Kluyveromyces marxianus under respiratory conditions. Sci. Rep. 9, 5319.
- Sanford, A., Kiriakov, S., Khalil, A.S., 2022. A toolkit for precise, multigene control in. ACS Synth. Biol. 11, 3912–3920.
- Schwartz, C., Frogue, K., Ramesh, A., Misa, J., Wheeldon, I., 2017a. CRISPRi repression of nonhomologous end-joining for enhanced genome engineering via homologous recombination in Yarrowia lipolytica. Biotechnol. Bioeng. 114, 2896–2906.
- Schwartz, C., Shabbir-Hussain, M., Frogue, K., Blenner, M., Wheeldon, I., 2017b. Standardized markerless gene integration for pathway engineering in yarrowia lipolytica. ACS Synth. Biol. 6, 402–409.
- Stemmer, M., Thumberger, T., Del Sol Keyer, M., Wittbrodt, J., Mateo, J.L., 2015. CCTop: an intuitive, flexible and reliable CRISPR/Cas9 target prediction tool. PLoS One 10, e0124633.
- Varanasi, U.S., Klis, M., Mikesell, P.B., Trumbly, R.J., 1996. The Cyc8 (Ssn6)-Tup1 corepressor complex is composed of one Cyc8 and four Tup1 subunits. Mol. Cell Biol. 16, 6707–6714.
- Vincent, A.C., Struhl, K., 1992. ACR1, a yeast ATF/CREB repressor. Mol. Cell Biol. 12, 5394–5405.
- Wade, J.T., Reppas, N.B., Church, G.M., Struhl, K., 2005. Genomic analysis of LexA binding reveals the permissive nature of the Escherichia coli genome and identifies unconventional target sites. Genes Dev. 19, 2619–2630.
- Weber, W., Fux, C., Daoud-el Baba, M., Keller, B., Weber, C.C., Kramer, B.P., Heinzen, C., Aubel, D., Bailey, J.E., Fussenegger, M., 2002. Macrolide-based transgene control in mammalian cells and mice. Nat. Biotechnol. 20, 901–907.
- Wittmann, A., Suess, B., 2012. Engineered riboswitches: expanding researchers' toolbox with synthetic RNA regulators. FEBS Lett. 586, 2076–2083.
- Yocum, R.R., Hanley, S., West Jr., R., Ptashne, M., 1984. Use of lacZ fusions to delimit regulatory elements of the inducible divergent GAL1-GAL10 promoter in Saccharomyces cerevisiae. Mol. Cell Biol. 4, 1985–1998.
- Zimran, G., Feuer, E., Pri-Tal, O., Shpilman, M., Mosquna, A., 2022. Directed evolution of herbicide biosensors in a fluorescence-activated cell-sorting-compatible yeast twohybrid platform. ACS Synth. Biol. 11, 2880–2888.